Interaction of Arrestin with Enolase1 in Photoreceptors

W. Clay Smith,[1,2] *Susan Bolch,*[1] *Donald R. Dugger,*[1] *Jian Li,*[1] *Isi Esquenazi,*[1] *Anatol Arendt,*[1] *Del Benzenhafer,*[1] *and J. Hugh McDowell*[1]

Purpose. Arrestin is in disequilibrium in photoreceptors, translocating between inner and outer segments in response to light. The purpose of this project was to identify the cellular component with which arrestin associates in the dark-adapted retina.

Methods. Retinas were cross-linked with 2.5 mM dithiobis(succinimidylpropionate) (DSP), and arrestin-containing complexes purified by anion-exchange chromatography. Tandem mass spectrometric analysis was used to identify the protein components in the complex. Enolase localization in photoreceptors was assessed by immunohistochemistry. Confirmation of interacting components was performed using immunoprecipitation and surface plasmon resonance (SPR). Enolase activity was also assessed in the presence of arrestin1.

Results. In retinas treated with DSP, arrestin cross-linked in a 125-kDa complex. The principal components of this complex were arrestin1 and enolase1. Both arrestin1 and -4 were pulled down with enolase1 when enolase1 was immunoprecipitated. In the dark-adapted retina, enolase1 co-localized with arrestin1 in the inner segments and outer nuclear layer, but remained in the inner segments when arrestin1 translocated in response to light adaptation. SPR of purified arrestin1 and enolase1 demonstrated direct binding between arrestin1 and enolase1. Arrestin1 modulated the catalytic activity of enolase1, slowing it by as much as 24%.

Conclusions. The results show that in the dark-adapted retina, arrestin1 and -4 interact with enolase1. The SPR data show that the interaction between arrestin1 and enolase1 was direct, not requiring a third element to form the complex. Arrestin1 slowed the catalytic activity of enolase1, suggesting that light-driven translocation of arrestin1 may modulate the metabolic activity of photoreceptors. (*Invest Ophthalmol Vis Sci.* 2011; 52:1832–1840) DOI:10.1167/iovs.10-5724

Rod and cone photoreceptors are highly specialized cells in the mammalian retina that capture photons and transduce light energy into a change in membrane potential that is ultimately relayed to the visual cortex. Photons are absorbed in these photoreceptors by opsin-based visual pigments to initiate the phototransduction cascade. The activity of the visual pigment is regulated by the arrestin family of proteins, 45-kDa proteins that sterically occlude access of transducin to the activated visual pigment until the vitamin A-derived chromophore is released and the rhodopsin is regenerated with 11-*cis* retinal (recently reviewed in Ref. 1).

Since arrestin functions to quench phototransduction, one would expect it to be primarily concentrated in photoreceptor outer segments where the visual pigment resides. Instead, the distribution of arrestin is quite dynamic, primarily localizing to the inner segments and perinuclear region of photoreceptors in the dark and then translocating to the outer segments during light adaptation.[2–6] This light-dependent change in arrestin distribution has been noted in both rods[4,7,8] and cones.[5,6,9] The function of arrestin translocation is unclear, although it has been hypothesized to have a role in adapting the photoreceptor's response to light, improving the temporal resolution of the photoresponse in background light.[3] Since the translocation occurs on a time scale that is relatively slow, however, an alternative hypothesis for the function of arrestin translocation is that it provides protection for rods against light-induced damage resulting from continuous operation of the phototransduction cascade.[10]

The mechanism of arrestin translocation has been investigated by various laboratories and revealed to be complex. It was originally proposed that arrestin translocation could be accounted for by a two-partner, diffusion-mediated model in which arrestin binds to activated rhodopsin in the outer segments in the light and microtubule elements in the inner segments in the dark.[11,12] The diffusion of arrestin through the connecting cilium is sufficiently fast to account for the translocation of arrestin in response to light.[13,14] However, it is clear that arrestin translocation is more complex, with a signaling cascade regulating the initial translocation of arrestin[15] and with more molecules of arrestin moving to the outer segments than the number of rhodopsin molecules bleached at threshold levels of light.[3] This initial signaling of arrestin translocation appears to be accomplished by a phospholipase C cascade.[15] In addition to this involvement of a signaling cascade, arrestin translocation also appears to be facilitated by cytoskeletal elements, with microtubules assisting in the distribution of arrestin to the apical end of the outer segments[16,17] and microfilaments facilitating the movement of arrestin from the outer segments to the inner segments.[17]

Although the evidence supporting arrestin binding to microtubules in vitro is quite strong,[18–20] the immunohistochemical data do not completely agree with tubulin/microtubules serving as the binding sink in the inner segments of dark-adapted rods. For example, binding of arrestin to microtubules in dark-adapted rod inner segments would be expected to generate a more linear or cross-hatched distribution of arrestin. This has not been observed in any of the studies of arrestin localization, whether studied by immunostaining[2,21] or direct observation of fluorescently tagged arrestin[2,13] or whether studied at the confocal[2,21] or ultrastructural level.[22] In all these studies, the distribution of arrestin is relatively uniform, occupying the available cytoplasmic volume of the inner segments.

From the Departments of [1]Ophthalmology and [2]Neuroscience, University of Florida, Gainesville, Florida.

Supported by Grants EY014864, EY06225, EY007132, and EY08571 from the National Eye Institute and by Research to Prevent Blindness. WCS is a recipient of the Research to Prevent Blindness Lew R. Wasserman Merit Award.

Submitted for publication April 16, 2010; revised August 23 and September 20, 2010; accepted September 20, 2010.

Disclosure: **W.C. Smith**, None; **S. Bolch**, None; **D.R. Dugger**, None; **J. Li**, None; **I. Esquenazi**, None; **A. Arendt**, None; **D. Benzenhafer**, None; **J.H. McDowell**, None

Corresponding author: W. Clay Smith, P.O. Box 100284, University of Florida, Gainesville, FL 32610-0284; wcsmith@ufl.edu.

Since arrestin appears to have a relatively uniform distribution in the cytoplasm of the rod inner segments, we initiated this study to determine whether the localization of arrestin to the inner segments in the dark-adapted state might be through a specific association with a protein or complex other than the microtubule cytoskeletal elements. Using cross-linking agents in dark-adapted retinas, we show that arrestin and enolase1 are cross-linked, suggesting that they interact. This interaction is confirmed in multiple manners, using immunoprecipitation, SPR, and an enolase activity assay. We demonstrate that this interaction is direct between the two molecules, not requiring any additional binding elements.

METHODS

Animals

The use of all animals and animal tissues was in accordance with the institutional guidelines of the University of Florida's Institutional Animal Care and Use Committee and the ARVO Statement for the Use of Animals in Ophthalmic and Vision Research.

Protein Cross-linking

A portion of a dark-adapted bovine retina (Lawson, Inc., Lincoln, NE) or freshly isolated, whole *Xenopus* retina was placed in 100 mM sodium phosphate buffer (pH 7.0) with 7.5 mM sodium chloride. Dithiobis(succinimidylpropionate) (DSP) in 100% DMSO was added to a final concentration of 2.5 mM in 10% DMSO (an equivalent volume of DMSO was added to the uncross-linked control sample). The solution was vortexed to disperse the retina and incubated at room temperature for 1 hour. The sample was thoroughly homogenized in a glass–glass homogenizer, and centrifuged (30,000*g*, 30 minutes, 4°C) to produce a cleared supernatant for Western blot analysis. For experiments investigating arrestin4, the pellet from this centrifugation was retained, resuspended in Laemmli's sample buffer, and also included for Western blot analysis.

In experiments for mass spectrometric identification of cross-linked proteins, the cross-linked supernatant was also purified over an anion-exchange resin (diethylaminoethyl-Sephacel; Sigma-Aldrich, St. Louis, MO), eluting with a 7.5- to 500-mM NaCl gradient. Fractions containing cross-linked arrestin1, as identified by Western blot analysis with an anti-arrestin1 antibody, were pooled, concentrated (Centri-Prep YM10; Millipore, Billerica, MA), and separated by 4% to 16% gradient SDS-PAGE (Bio-Rad, Hercules, CA). After visualization with Coomassie blue, the band containing cross-linked arrestin1 was excised and subjected to LC-MS/MS. Nonreducing sample buffer was used for all samples to preserve the DSP-mediated cross-links.

For Western blot analysis, gels were transferred to PVDF membrane (Millipore) in methanolic Tris-glycine buffer. Membranes were blocked with 1% low immunoglobulin fetal bovine serum (Invitrogen, Carlsbad, CA) in PBS, and probed with primary antibody in the same blocking buffer. For this study, we used anti-arrestin1 monoclonal antibodies SCT-128 (epitope 300-320 of arrestin1[23]) and S65-38 (epitope 380-404 of arrestin1[24]), anti-enolase1 monoclonal antibody Enol2-81 (amino terminus of bovine enolase1 as described below), anti-enolase1 polyclonal antibody NB100 (Novus Biologicals, Littleton, CO), anti-arrestin4 monoclonal antibody xCAR2–166,[25] anti-enolase2 monoclonal antibody (sc-21738; Santa Cruz Biotechnology, Santa Cruz, CA), anti-aldolase antibody (Rockland Immunochemicals, Inc., Gilbertsville, PA), anti-glutamate dehydrogenase antibody (Rockland), and anti-lactate dehydrogenase antibody (Rockland). Species-specific secondary antibodies complexed with alkaline phosphatase were used to detect the primary antibody using nitro blue tetrazolium chloride/ 5-bromo-4-chloro-3-indolyl phosphate as a substrate.

Liquid Chromatography-Tandem Mass Spectrometry

Coomassie blue–stained bands were excised from polyacrylamide gels (for both *Xenopus* and bovine samples), digested with trypsin, injected onto a capillary trap (LC Packings PepMap; Dionex, Sunnyvale, CA) and desalted for 5 minutes with a 10-mL/min flow rate of 0.1% vol/vol acetic acid. The samples were loaded onto a C18 HPLC column (LC Packings PepMap; Dionex). The elution gradient of the HPLC column started at 3% solvent A and 97% solvent B and finished with 60% solvent A and 40% solvent B for 60 minutes for protein identification (solvent A: 0.1% vol/vol acetic acid, 3% vol/vol acetonitrile, and 96.9% vol/vol water; solvent B: 0.1% vol/vol acetic acid, 96.9% vol/vol acetonitrile, and 3% vol/vol water). LC-MS/MS analysis was performed on a hybrid quadrupole-TOF mass spectrometer (QSTAR; Applied Biosystems, Inc. [ABI], Framingham, MA). The focusing potential and ion spray voltage were set to 275 and 2600 V, respectively. The information-dependent acquisition (IDA) mode of operation was used in which a survey scan from m/z 400 to 1200 was acquired, followed by collision-induced dissociation of the three most intense ions. Survey and MS/MS spectra for each IDA cycle were accumulated for 1 and 3 seconds, respectively.

Protein Search Algorithm

Tandem mass spectra were extracted (Analyst version 1.1; ABI). All MS/MS samples were analyzed using Mascot (ver. 2.0.01; Matrix Science, London, UK). Mascot was set up to search the NCBInr database assuming trypsin as the digestion enzyme (Mascot is available in the public domain at www.matrix.com). Mascot was searched with a fragment ion mass tolerance of 0.30 Da and a parent ion tolerance of 0.30 Da. Iodoacetamide derivative of Cys, deamidation of Asn and Gln, and oxidation of Met were specified in Mascot as variable modifications. Protein identification software (Scaffold, ver. 01-06-03; Proteome Software Inc., Portland, OR) was used to validate MS/MS-based peptide and protein identification. Peptide identifications were accepted if they could be established at greater than 95.0% probability as specified by the Peptide Prophet algorithm.[26] Protein identifications were accepted if they could be established at greater than 99.0% probability and contained at least two identified unique peptides. Protein probabilities were assigned by the Protein Prophet algorithm.[27]

Antibody Preparation

A 12-amino-acid peptide from bovine enolase1 N terminus (MSILKLVAREIF) was synthesized at 0.1 mmol scale, by solid phase, using Fmoc derivatives of amino acids, with automatic synthesizer (model 431A; ABI). Multiple copies of the peptides were synthesized on an inert lysine core with eight-branched MAPS resin (Ana Spec, San Jose, CA), after the DCC/HOBt protocol. The completed peptide was cleaved from resin using 95% trifluoroacetic acid with 2.5% triisopropylsilane and 2.5% water for 2 hours. The peptide was precipitated from solution using cold diethyl ether and lyophilized.

The octamer peptide or full-length His (6)-tagged bovine enolase1 purified from yeast (described below) was dissolved in phosphate-buffered saline and injected into BALB/c mice for the production of monoclonal antibodies. Hybridoma fusions were cloned and screened against purified full-length bovine enolase1, 2, and 3 that were heterologously expressed in bacteria to identify monoclonal antibodies that were specific to enolase1. To obtain the enolase isoforms, cDNAs for bovine enolase1, -2, and -3 were amplified from bovine retinal poly(A)$^+$ RNA that had been reverse transcribed after priming with oligo(dT). PCR primers were used that incorporated *Eco*RI sites flanking the open reading frame. The 5′ primer also incorporated a His(6) tag between the initiating methionine codon and second codon. Bovine enolases were cloned into the *Eco*RI site of pET-28a (Novagen, Madison, WI), and expressed in the BL21(DE3) strain of *Escherichia coli*. Cultures were grown overnight at 30°C with 30 μM isopropyl β-D-1-thiogalactopyranoside to induce expression of the enolases. Bacterial cultures were disrupted with a French press (20,000 psi) in 50 mM sodium phosphate buffer with 300 mM NaCl and 10 mM imidazole (pH 8.0), and the enolase purified to >95% homogeneity by affinity purification on a His column (Gravi-Trap; GE Life Sciences, Piscataway, NJ), eluting with the same buffer containing 500 mM imidazole. Eluted samples

were dialyzed against phosphate-buffered saline. Hybridomas Enol1-8, Enol2-81, and Enol2-53 were tested against heterologously expressed bovine enolase1, -2, and -3 and shown to be specific for enolase1 (Supplementary Fig. S1, http://www.iovs.org/lookup/suppl/doi:10.1167/iovs.10-5724/-/DCSupplemental).

Immunoprecipitation

Samples of bovine retina treated as above with 2.5 mM DSP (or DMSO as a non–cross-link control) were immunoprecipitated using protein G-coated magnetic beads (Dynal; Invitrogen). The beads were loaded with purified anti-enolase1 monoclonal antibody (Enol1-8) or with anti-enolase2 monoclonal antibody (SC-21738; Santa Cruz Biotechnology); beads with no antibody or with anti-transducin α-subunit antibody (SC-389; Santa Cruz Biotechnology) were used as controls for non-specific binding. Retinal extracts were applied to the beads, incubated for 1 hour (25°C), and then captured magnetically. After washing the beads in phosphate buffer, bound protein was eluted with Laemmli sample buffer and subjected to Western blot analysis. All immunoprecipitation procedures were performed using dark-adapted bovine retinas in dim red illumination. Blots were probed with anti-enolase1 (Eno12-81), anti-arrestin1 (SCT-128), anti-arrestin4 (xCAR2-166), anti-transducin,[16] or anti-tubulin (SC-5546; Santa Cruz Biotechnology) antibodies.

Immunohistochemistry

Wild-type *Xenopus laevis* tadpoles were either dark adapted overnight or exposed to laboratory lighting (800 lux) for 1 hour and then fixed in methanolic formaldehyde as previously described.[2] Cryosections were probed with an anti-enolase1 monoclonal antibody (Enol2-53, IgG_1) and a mouse anti-arrestin monoclonal antibody (XAR1–6,[2] IgG_{2b}). Anti-isotype-specific secondary antibodies were used to detect the primary antibodies, using anti-mouse IgG_{2b}-Texas red and anti-mouse IgG_1-AlexaFluor 488 (Invitrogen). Nuclear DNA was stained with 4′,6-diamidino-2-phenylindole (Invitrogen).

Protein Purification for SPR and Biochemical Assays

To obtain enolase that was free of all extraneous sequence, except for an N-terminal His (6) tag, bovine enolase1 cDNA was excised from the above-described pET-28 expression vector with *Eco*RI, cloned into the *Eco*RI site of pPIC-ZA (Invitrogen), and stably recombined into the *Pichia* genome. Yeast cultures were disrupted with a French press (20,000 psi) in 50 mM sodium phosphate buffer with 300 mM NaCl and 10 mM imidazole (pH 8.0), and the enolase purified to >95% homogeneity by affinity purification on a His column (Gravi-Trap; GE Life Sciences), eluting with the same buffer containing 500 mM imidazole. Eluted samples were dialyzed against 15 mM Tris-HCl (pH 7.4) with 1 mM $MgCl_2$, 1 mM $CaCl_2$, and 0.1 mM DTT, and stored at −80°C.

Bovine arrestin1 was either purified from bovine retinal homogenates as described elsewhere,[28] and subsequently modified,[29] or was purified from *Pichia pastoris* where it was expressed with an N-terminal His (6) tag, as previously described.[30,31] To control for potential effects from small amounts of contaminating proteins, we subjected an extract from nonrecombinant *Pichia* (strain GS115) to the identical purification procedure and used in the catalytic assay described below.

Surface Plasmon Resonance

All SPR data were collected on a protein-interaction analysis system (Biacore 3000 GE Healthcare). Arrestin1, purified from bovine retinas, was immobilized to a sensor chip (Biacore CM4; GE Healthcare) via amine coupling, by using the immobilization wizard according to the manufacturer's manuals. The carboxylated dextran matrix on the sensor chip surface was equilibrated with 50 mM $NaPO_4$, 50 mM NaCl (pH 7.0) containing 0.01% P20 surfactant (GE Life Sciences). The carboxyl groups were then activated with a 50 mM N-hydroxysuccinimide (NHS) and 200 mM *N*-ethyl [(dimethylamino)propyl]carbodiimide. Arrestin1, diluted 1:20 with sodium acetate buffer (pH 5.5) to a concentration of 43 μM, was used for linking to the surface at 1000 refractive units (RU). The remaining activated carboxyl groups were blocked by reacting with 1 M triethylamine (pH 8.5).

The interaction between enolase1 and arrestin1 was monitored by SPR (BIAcore 3000; GE Healthcare). Enolase1 prepared as just described from *Pichia* was dialyzed against 50 mM $NaPO_4$, 50 mM NaCl, 1 mM $MgCl_2$ (pH 7.0) containing 0.05% Tween 20. The dialysis buffer was used as the running buffer in the experiments. For regeneration of the surface, 50 to 150 μL of regeneration solution (50 mM $NaPO_4$, 1.05 M NaCl, 1 mM $MgCl_2$ [pH 7.0], containing 0.05% Tween 20) was injected at the end of each analysis cycle.

Enolase Catalytic Activity

The enzymatic activity of enolase1 was measured by monitoring the loss of absorbance at 340 nm, as NADH is oxidized when 2-phosphoglycerate is converted to lactic acid.[32] Briefly, bovine enolase1 (purified from *Pichia*) was dialyzed into 15 mM Tris-HCl with 1 mM $MgCl_2$, 1 mM $CaCl_2$, and 0.1 mM DTT (pH7.4). Enolase1 was added at a final concentration of 77 nM to a reaction mix containing 2 mM 2-phosphoglycerate, 3 U/mL pyruvate kinase (Sigma-Aldrich), and 3.6 U/mL lactate dehydrogenase (Sigma-Aldrich) in 15 mM Tris-HCl with 25 mM $MgSO_4$, 100 mM KCl, 0.2 mM NADH, 2 mM ADP, 0.02% (wt/vol) bovine serum albumen, and 0.01% P20 surfactant. In some experiments, bovine arrestin1 purified from heterologous expression in yeast was added in increasing amounts (0–32 μM). The reaction mix was prewarmed to 25°C and maintained at 25°C in a Peltier-controlled cuvette holder during the 10-minute reaction time. The rate of enolase activity was determined from a linear fit of the decline in absorbance at 340 nm for data collected at 1-minute intervals over 1 to 10 minutes. To control for effects contributed by contaminating components in the purified protein preparations, we used an extract prepared from nonrecombinant yeast (described above) in volumes equivalent to that used for arrestin1.

Results

Cross-linking of Arrestin in Retina

Studies have shown that arrestin1 is in disequilibrium in dark-adapted rod photoreceptors, primarily localizing to the rod inner segments.[2–4] This distribution was unexpected, given arrestin's high cytosolic solubility. In an effort to identify the cellular component(s) that might maintain this disequilibrium in the dark-adapted rod, we attempted to cross-link arrestin1 in situ using DSP to form a stable complex of arrestin1 with the proteins in near proximity. Figure 1A shows a Western blot stained with an anti-arrestin1 monoclonal antibody, comparing extracts of untreated bovine retina (lane 1) with an extract from a retina treated for 1 hour with DSP cross-linker (lane 2). In the untreated retina, a prominent doublet was present at 48 and 44 kDa, representing full-length arrestin and its shorter splice variant form.[33] In the retina treated with DSP cross-linker, an additional doublet was detected at ~110 and 125 kDa. A similar complex at 125 kDa was formed in retinas from adult *Xenopus* treated with the DSP cross-linker (see Fig. 3A).

To identify the components of this higher-molecular-mass band, we prepared soluble extracts separately from both bovine and *Xenopus* retinas that were cross-linked with 2.5 mM DSP in phosphate buffer, and the soluble components purified using DEAE anion-exchange chromatography. Fractions containing the higher-molecular-mass product (as determined by anti-arrestin1 Western blot analysis) were separated on 4% to 15% gradient SDS-PAGE, and although they contained a complex mixture of proteins, a distinct band was visible at 125 kDa with Coomassie blue staining that corresponded to the band recognized by the anti-arrestin1 antibody on Western blot (Fig.

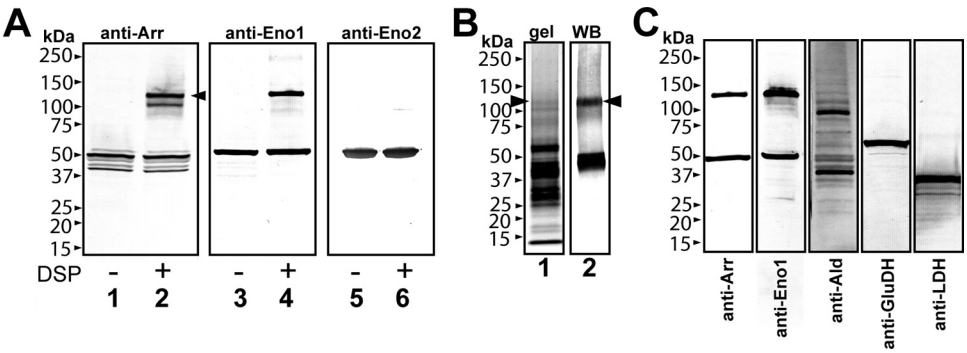

FIGURE 1. Arrestin-containing complexes in retina cross-linked with DSP. (**A**) Western blot of retinal extracts prepared from dark-adapted bovine retina treated with 10% DMSO only (*lanes 1*, *3*, *5*) or with 2.5 mM DSP in 10% DMSO (*lanes 2*, *4*, *6*). Replicate blots were probed with anti-arrestin1 monoclonal antibody SCT-128 (*lanes 1, 2*), with anti-enolase1 antibody NB100 (*lanes 3, 4*), or with anti-enolase2 antibody SC-21738 (*lanes 5, 6*). *Arrowhead*: an arrestin1-containing complex at 125 kDa. (**B**) Coomassie blue–stained gel (*lane 1*) and corresponding Western blot (*lane 2*) of extracts prepared from DSP cross-linked bovine retinas that were fractionated by anion-exchange chromatography; Western blot strip (*lane 2*) was probed with anti-arrestin SCT-128 antibody. *Arrowheads*: the 125-kDa complex. (**C**) Western blot analysis of replica strips of bovine retina treated with 2.5 mM DSP. The strips were probed with antibodies against arrestin1 (S65-38), enolase1 (Enol2-81), aldolase C, glutamate dehydrogenase, or lactate dehydrogenase.

1B shows the fraction obtained from the bovine extract). The 125-kDa band was excised, and subjected to tandem MS/MS analysis to identify the protein components. Table 1 shows the data obtained from this analysis, listing all proteins for which at least two peptides were identified for any given protein for each species. The two most prevalent peptides identified were for enolase1 and arrestin1 in both *Xenopus* and bovine extracts (note that both trypsin and keratin are common contaminants from the MS/MS process). To verify that the 125-kDa band is in fact a complex of both arrestin1 and enolase1, a Western blot of cross-linked and non–cross-linked bovine retinal samples was probed with an anti-enolase1-specific antibody (Fig. 1A, lanes 3, 4 for bovine; Fig. 3A, lanes 3, 4 for *Xenopus*). This antibody reacted with both a 50-kDa band (the expected size of monomeric enolase) and the 125-kDa band, which is also recognized by the anti-arrestin1 antibody. To determine whether this cross-linking is specific for the enolase1 isoform of enolase, we probed a replica blot with an enolase2-specific antibody (Fig. 1A, lanes 5, 6). Enolase2 immunoreactivity was noted only at the monomeric 50-kDa size and none at the 125-kDa range.

Although peptides matching enolase1 and arrestin1 were most prevalent in the 125-kDa band, several other proteins were also identified that were represented by at least two peptides in the two different species: aldolase C, glutamate dehydrogenase, and lactate dehydrogenase. The presence of these proteins in the 125-kDa complex was determined by Western blot analysis of cross-linked bovine retinal samples, probed with antibodies specific for each of these proteins (Fig. 1C). Although each antibody reacted with at least one band in the extract, none of the antibodies reacted with the 125-kDa band in which both arrestin1 and enolase1 were present. The lack of correspondence with the 125-kDa band suggests that these other proteins identified by mass spectrometry are simply nonspecific contaminants.

Since cross-linking has the potential to artificially link proteins that are in very close proximity, but without any direct association, the interaction between enolase1 and arrestin1 was confirmed by immunoprecipitation with an anti-enolase1 antibody (Fig. 2). Bovine retinas that had been treated with 2.5 mM DSP cross-linker or left untreated were incubated with magnetic beads coated with protein G and Enol1-8 monoclonal antibody. Western blot analysis of the precipitated material showed that the enolase1 antibody captured both enolase1 (Fig. 2A) and arrestin1 (Fig. 2B). Importantly, arrestin1 was pulled down, even in retinal extracts that had not been stabilized by the DSP cross-linker. To determine whether tubulin was also immunoprecipitated with enolase1 and arrestin1, a replica blot was probed with anti-tubulin antibody (Fig. 2C). No reactivity was noted, even though the control (Fig. 2C, inset) showed that the anti-tubulin antibody recognizes a robust band in the whole retinal extract. The association between arrestin1 and enolase appears to be specific for the enolase1 isoform, since immunoprecipitation with an enolase2-specific antibody did not pull down any arrestin1 (Fig. 2D); the control blot developed with an enolase2 antibody demonstrates that the enolase2 antibody was effective at pulling down enolase2 (Fig. 2E). Additional control blots without any precipitating antibody (Figs. 2F, 2G) or with an irrelevant

TABLE 1. Proteins Identified by Tandem MS/MS Analysis of a 125-kDa Band Isolated from *Xenopus* and Bovine Retinas Cross-linked by DSP

Identified Protein	Molecular Mass (kDa)	Number of Peptides		Percent Coverage of Protein	
		Xenopus	Bovine	*Xenopus*	Bovine
Enolase 1	47	10	11	47	32
Arrestin 1	45	7	6	26	18
Keratin 1	66	11	4	24	12
Trypsin, chain A	23	3	3	17	8
Aldolase C	39	2	4	9	5
Glutamate dehydrogenase 1	60	4	3	8	9
Lactate dehydrogenase A1	36	2	—	8	—
Glyceraldehyde 3-P dehydrogenase	36	—	2	—	8

All proteins that were identified by at least two peptides (>95% sequence match/peptide) are listed.

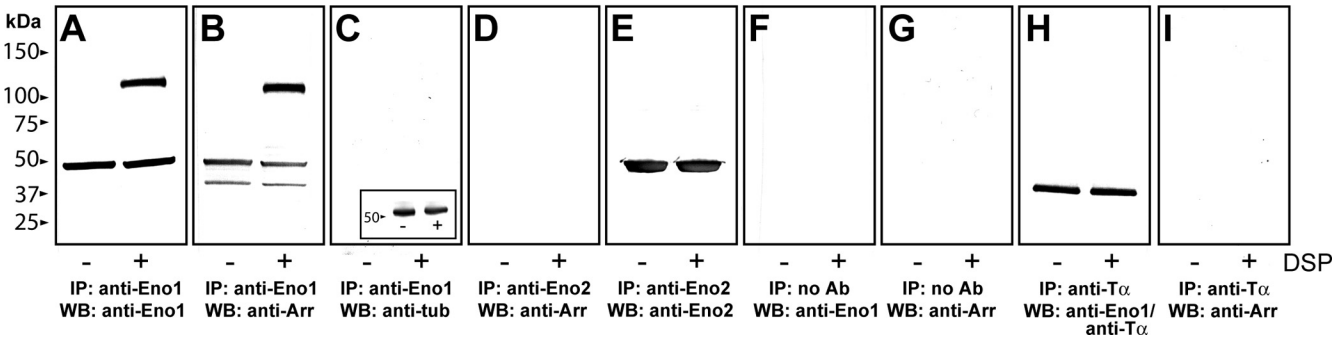

Figure 2. Arrestin co-immunoprecipitates with enolase1. Bovine retinal extracts were either treated with DSP cross-linker (+) or 10% DMSO (−) and then immunoprecipitated with protein-G magnetic beads complexed with anti-enolase1 antibody (**A**–**C**), anti-enolase2 antibody (**D**, **E**), no antibody (**F**, **G**), or anti-transducin-α antibody (**H**, **I**). Captured proteins were eluted with SDS sample buffer and probed on Western blot analysis with anti-enolase1 (Enol2-81; **A**, **F**), anti-arrestin1 (SCT-128; **B**, **D**, **G**, **I**), anti-tubulin (SC-5546; **C**), anti-enolase2 (SC-21738; **E**), or a mixture of anti-enolase1 (Enol2-81) and anti-transducin α (SC-389; **H**). (**C**, *inset*) A Western blot of whole retina extract probed with the same anti-tubulin antibody, to demonstrate that the antibody recognizes tubulin in the bovine retina.

anti-transducin-α antibody (Fig. 2H, 2I) did not pull down enolase1 or arrestin1.

To test whether the association of arrestin1 with enolase1 is dependent on the illumination conditions, we used adult *Xenopus* retinas, since the lighting conditions can be readily manipulated in the laboratory. Fresh retinas were isolated from adult *Xenopus* and then cross-linked with 2.5 mM DSP after the eyes had been either dark adapted for 3 hours or light adapted for 45 minutes (Fig. 3B). The 125-kDa complex was present only in extracts prepared from the dark-adapted eye.

Enolase Immunolocalization in Retina

To determine whether enolase1 co-localized with arrestin in the photoreceptors, cryosections of *Xenopus* tadpole eyes were immunoprobed with an anti-enolase1 and anti-arrestin1 antibodies. In the dark-adapted *Xenopus* retina (Figs. 3C–E), enolase1 immunoreactivity was most abundant over the inner segments, the region surrounding the nuclei, the nuclei of rod and cone photoreceptors, and the outer plexiform layer (Fig. 3C). This distribution of enolase1 significantly overlapped that of arrestin1 in the dark-adapted retina (Fig. 3D). In the light-

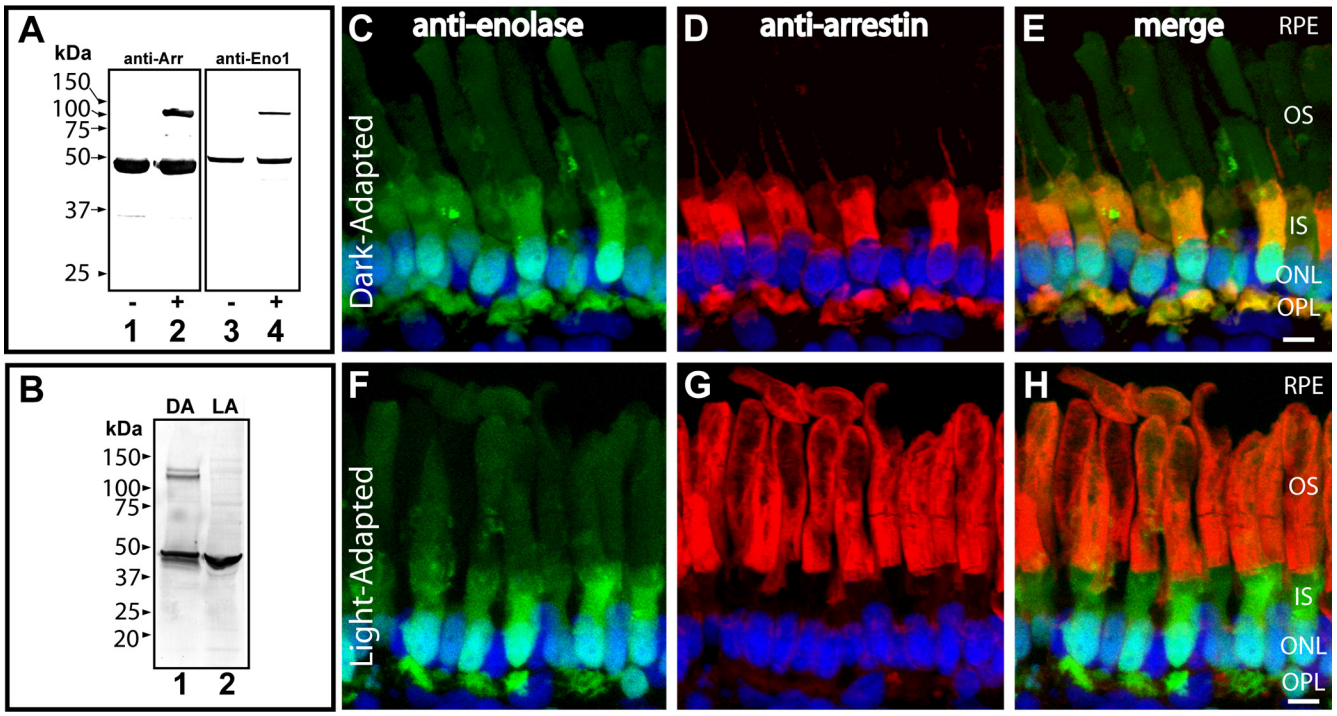

Figure 3. Cross-linking and immunohistochemical localization of enolase1 in *Xenopus* retina. (**A**) Retinas from *Xenopus* adults were treated with 2.5 mM DSP (*lanes 2*, *4*) or with 10% DMSO (*lanes 1*, *3*). Replica blots were probed with anti-arrestin1 (XAR1–6) or with anti-enolase1 (Enol2-53). (**B**) Western blot of retinal extracts prepared from adult *Xenopus* retinas that were dark adapted 3 hours (*lane 1*) or light adapted 45 minutes (*lane 2*) before 2.5 mM DSP was added. The blot was probed with anti-arrestin1 antibody SCT-128. (**C**–**H**) Immunolocalization of enolase1 and arrestin1 in (**C**–**E**) dark- or (**F**–**H**) light-adapted *Xenopus* tadpole eyes. Cryosections were stained for enolase1 (*green*) using anti-enolase1 antibody (Enol2-53) or arrestin1 (*red*) using anti-arrestin1 antibody (XAR1-6). Nuclear DNA was stained with DAPI (*blue*). RPE, retinal pigmented epithelium; OS, outer segments; IS, inner segments; ONL, outer nuclear layer; OPL, outer plexiform layer. Scale bar, 10 μm.

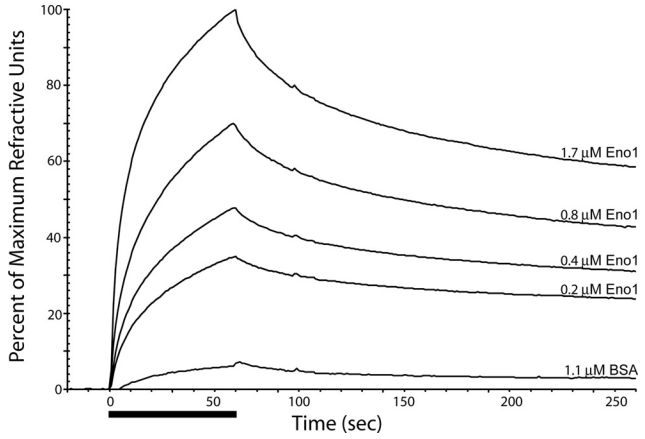

FIGURE 4. SPR analysis of arrestin1 and enolase1 interaction. Bovine arrestin1 was immobilized on the surface of a CM4 chip, and the indicated concentrations of enolase1 (0.2–1.7 μM) were flowed across its surface (*horizontal bar* below the *x*-axis indicates the period during which enolase1 was injected). BSA (1.1 μM) was also injected as a negative control.

adapted frog retina (Figs. 3F–H); however, most of the arrestin1 translocates to the outer segments (Fig. 3G), whereas the enolase1 remains in the inner segments and outer nuclear layer and does not appear to have an altered distribution (Fig. 3F). In addition to the presence of enolase1 in the inner segment region of the photoreceptors, a smaller, but detectable portion of immunofluorescence is also present in the outer segments (approximately 10% of the total fluorescence).

Enolase/Arrestin Interaction

To further characterize the interaction between arrestin1 and enolase1, we performed SPR studies on purified samples of arrestin1 isolated from bovine retinas and recombinant bovine enolase1 expressed in *Pichia* (Fig. 4). Various concentrations of enolase1 were flowed over arrestin1 immobilized on the chip surface for 60 seconds, followed by continuous flow of buffer. Binding of enolase1 to arrestin1 is indicated by the increase in refractive units (RU) observed as enolase1 is applied to the chip. As increasing concentrations of enolase1 are added, the RU increases in an approximately proportional manner. The binding and release curves for the interaction are complex such that it is not possible to calculate on or off rates, nor equilibrium constants. As a negative control, bovine serum albumin (BSA) was injected at a concentration nearly equal to the highest enolase1 concentration used in this assay. Under these conditions, very little binding was observed with BSA, thus indicating that the interaction of arrestin1 and enolase1 is specific.

To determine whether there was a conformational component to the interaction of arrestin1 and enolase1, we injected enolase1 at 0.83 μM for various times (data not shown). The release kinetics for all injections times were nearly identical, indicating that conformational changes do not contribute to the binding of arrestin1 and enolase1.

Effects of Arrestin on Enolase Enzymatic Activity

Enolase is a glycolytic enzyme, functioning as a dehydrogenase converting 2-phosphoglycerate to phosphoenolpyruvate. In light of the direct interaction between enolase1 and arrestin1 identified by SPR, we next investigated whether arrestin1 modulates the catalytic activity of enolase1. In this assay, 77 nM enolase1 was mixed with 2-phosphoglycerate in the presence or absence of arrestin. Consumption of NADH was measured as an assay for the activity of enolase1. Figure 5 shows that under the conditions of our assay, the purified enolase1 catalyzes the hydrolysis of 2-phosphoglycerate at a rate of 2.55 mmol $\cdot$ $min^{-1} \cdot g^{-1}$ of enolase1. This catalytic activity is significantly slowed, however, by the addition of excess arrestin, approaching an asymptotic level of 1.92 mmol $\cdot$ $min^{-1} \cdot g^{-1}$. This difference represents a 24.7% reduction of the enolase1 activity in the presence of a 400-fold excess of arrestin1. The concentrations of arrestin1 and enolase1 used in this assay are significantly below the physiological concentrations, with arrestin1 being present in rod photoreceptors at ~1 mM, and enolase1 being approximately fivefold less at ~200 μM.[3,34–36] Since we are using heterologously expressed and purified bovine arrestin1 from *Pichia*, the possibility exists that a minor contaminating component could be the source of this inhibitory effect. To address this possibility, we repeated the assay using an extract of nonrecombinant *Pichia* prepared in the same manner as we purify the bovine arrestin1. No effect on enolase catalytic activity was noted (data not shown).

Association of Enolase1 with Arrestin4

Since enolase1 is present in both rod and cone photoreceptors, we investigated whether enolase1 might also interact with arrestin4. Bovine retinal extracts were treated as previously described, by incubated with 2.5 mM DSP or carrier and then separating the extract into aqueous soluble and insoluble components by centrifugation. Replica Western blot analysis of these samples (Figs. 6A–C) show that the monomeric form of arrestin1 and the 125-kDa complex containing arrestin1 remain in the soluble fractions (Fig. 6A, lanes 1, 2). In contrast, arrestin4 moves to the aqueous-insoluble fraction in the presence of DSP, as does a second band containing arrestin4 at 125 kDa (Fig. 6B). When this blot is probed for the presence of enolase1, enolase1 immunoreactivity is noted not only in the aqueous-soluble sample at both 50 and 125 kDa, but also in the aqueous-insoluble fraction of the DSP sample at both 50 and 125 kDa (Fig. 6C). This observation prompted us to reinvestigate our immunoprecipitation experiment using a total retinal homogenate rather than simply the aqueous soluble fraction. Using an anti-enolase1 antibody as the precipitating antibody, arrestin4 could be detected in the immunoprecipitate in samples, both with and without DSP cross-linker (Fig. 6D, lanes 13,

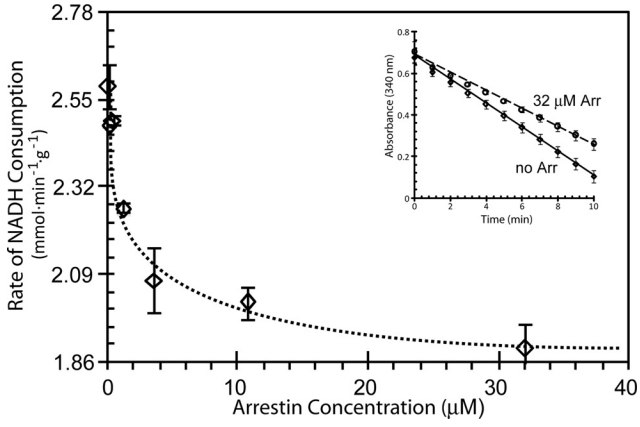

FIGURE 5. Modulation of enolase1 catalytic activity by arrestin. Enolase1 enzymatic activity was assessed in a biochemical assay, measuring the rate of NADH consumption (loss of OD_{340nm}) as 2-phosphoglycerate is converted to lactate. Enolase1 activity was assayed in the presence of increasing concentrations of arrestin1; data points represent the average (±SEM), $n = 6$. *Inset*: average traces of the raw data used to calculate the rates of enolase activity in the absence or presence of 32 μM arrestin1.

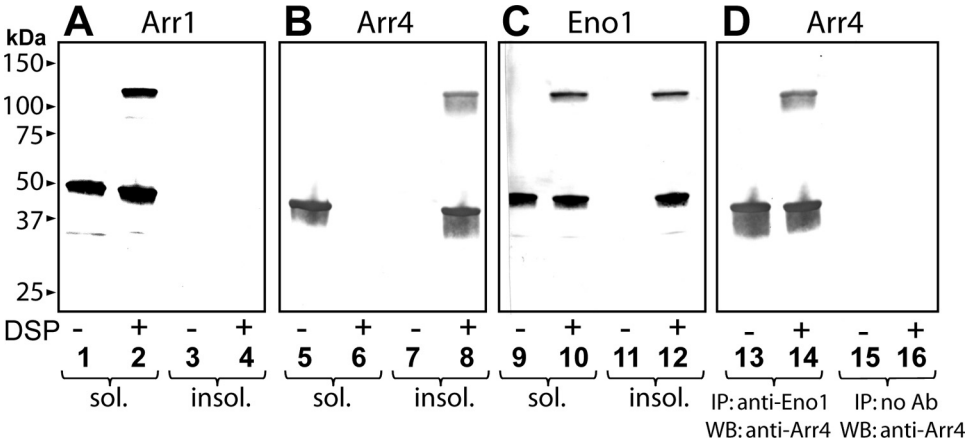

Figure 6. Interaction of arrestin4 with enolase1. (**A–C**) Replica Western blot analysis of bovine retina prepared with (+) or without (−) 2.5 mM DSP; samples were separated into aqueous-soluble and -insoluble fractions by centrifugation and probed with (**A**) anti-arrestin1 (SCT-128), (**B**) anti-arrestin4 (xCAR2-166), or (**C**) anti-enolase1 (Enol2-81). (**D**) Western blot of bovine retinal extracts immunoprecipitated with either anti-enolase1 antibody (*lanes 13*, *14*) or with no antibody (*lanes 15*, *16*). The blot was probed with arrestin4-specific monoclonal xCAR2-166.

14). A control immunoprecipitation with no antibody did not contain any arrestin4 immunoreactivity (Fig. 6D, lanes 15, 16).

Discussion

This study reveals a previously unrecognized interaction between the visual arrestins and enolase1. Although this discovery was initially made using in situ cross-linking via DSP which can artificially stabilize proteins within 1.5 Å distance, the validity of the interaction was established using three additional approaches: (1) immunoprecipitation of arrestin via anti-enolase1 antibodies, (2) measurement of enolase1 binding to arrestin1 via SPR, and (3) measurement of enolase1 catalytic activity in the presence of arrestin1. It is significant that immunoprecipitation of enolase1 pulled down arrestin1 even in the absence of DSP cross-linker, indicating that the association between arrestin1 and enolase1 is not artificially generated by the cross-linker. Importantly, our studies using SPR with purified enolase1 and arrestin1 provide a clear demonstration that these two proteins directly interact without requiring any additional scaffolding elements. These results, in their totality, provide convincing evidence that enolase1 interacts with arrestin1. It is significant that these observations were also replicated in two species (cow and *Xenopus*), indicating a broad species relevance for the interaction between arrestin1 and enolase1.

The interaction of arrestin1 with enolase is apparently specific for the enolase1 isoform based on the following evidence. First, enolase2 was not identified in our tandem mass spectrometric analysis of the cross-linked complex, nor was it detected in the complex by Western blot analysis. In addition, immunoprecipitation of enolase2 did not pull down any arrestin1 under the same conditions where enolase1 pulled down arrestin1.

Our discovery of this direct interaction between enolase1 and arrestin1 is a new finding. The only previous link between these two proteins is a study showing that arrestin1 co-purified with several glycolytic enzymes, including enolase1 and -2, when using hydroxyapatite agarose chromatography.[37] No evidence was provided, however, that would distinguish whether this co-purification was coincidental or whether these proteins were co-purifying as a complex.

In addition to our discovery that enolase1 interacts with arrestin1, our data also suggest that a similar interaction occurs with arrestin4. The supporting evidence is twofold (Fig. 6): First, enolase1 cross-linked to arrestin4 in the presence of DSP. Unlike the complex formed with arrestin1, the enolase1/arrestin4 complex was aqueous insoluble. This shift in solubility likely explains why arrestin4 was not identified as one of the potential binding partners by mass spectrometric analysis since only the soluble fraction was retained for enrichment by anion-exchange chromatography. The second supporting line of evidence is that arrestin4 was immunoprecipitated by enolase1. Although the evidence for the interaction of arrestin4 with enolase1 is not as complete as we have developed for arrestin1, the association does appear to be credible.

Immunolocalization of enolase1 in the outer retina indicates that enolase1 shares a significant overlap with arrestin1 in dark-adapted rod photoreceptors, primarily in the inner segments and outer nuclear layer. In these regions, the distribution of enolase1 is diffuse, similar to that of arrestin. The localization of enolase1 is consistent with that of other glycolytic enzymes (e.g., glyceraldehyde-3-phosphate dehydrogenase and lactate dehydrogenase) which are principally localized to the inner segments and outer nuclear layer, but with a smaller portion localized in the outer segments.[38] In addition to the co-localization with arrestin1, enolase is also significantly localized to the nuclei of rods and cones. This nuclear localization for enolase1 has been documented in other tissues where enolase1 serves as a transcription repressor.[39]

It is curious that in both our cross-linking and immunoprecipitation studies, we did not find an association of arrestin1 with tubulin, as has been documented.[11,18,19] Several possible explanations can be envisioned. For the cross-linking studies, it is simply possible that arrestin is not oriented in such a way with the microtubules to permit cross-linking by the DSP cross-linker. For the immunoprecipitation, a possible explanation is that since we are capturing arrestin1 that is associated with enolase1, tubulin may be sterically occluded from binding to arrestin, or we may be capturing a different population of arrestin molecules than those associated with microtubules. Alternatively, the affinity of arrestin to tubulin may be sufficiently low that tubulin would not remain associated with arrestin during the washes of the magnetic beads.

While the manuscript for this article was under review, a report was published identifying a new interaction between arrestin1 and *N*-ethylmaleimide-sensitive factor (NSF).[40] NSF was not identified as a binding partner for arrestin1 in our study for the following possible reasons: First, since NSF is primarily localized to the synaptic regions of the photoreceptors and enolase1 is found throughout the photoreceptor inner segments, it is possible that our immunoprecipitation of enolase1 was pulling down a different subcellular fraction of arrestin1 than that bound to NSF. Alternatively, binding of enolase1 to arrestin1 may block binding by NSF, thus preventing the concomitant immunoprecipitation of both arrestin1 and NSF with anti-enolase1 antibodies. With regard to why NSF was not identified in our mass spectroscopic analyses, in our study, we purified only the population of arrestin1 that was cross-linked into a larger complex. The absence of NSF in the complex suggests that when NSF is bound to arrestin1, it is not oriented in such a way that the DSP cross-linking agent can form an amide bond.

Modulation of Glycolysis by Arrestin

Enolases are a family of 48-kDa proteins that catalyze the dehydration of 2-phospho-D-glycerate to phosphoenolpyruvate in glycolysis. There are three isozymes— enolase1 (α-enolase), enolase2 (γ-enolase), and enolase3 (β-enolase)—that function as obligate homo- or heterodimers. Typically, enolase1 is broadly expressed in a variety of tissues, enolase2 is specific to neurons and neuroendocrine tissue, and enolase3 is found nearly exclusively in muscle.[41] In contrast to arrestin1, enolase1 does not show any changes in distribution in response to light adaptation, indicating that lighting conditions could therefore modulate the interaction between these two proteins. This conjecture is supported by our cross-linking studies which show a dramatic reduction in cross-linking between arrestin1 and enolase1 in samples that have been light adapted (Fig. 3B).

Our studies indicate that interaction with arrestin1 modulates the activity of enolase1, reducing the catalytic rate by as much as 25%. Since the energetic demands of photoreceptors are enormous, estimated to be on the order of 10^8 ATP $\cdot$ s^{-1} $\cdot$ $cell^{-1}$,[42] this modulation of enolase catalysis has potentially important implications. In the dark, nearly all of the ATP is consumed in pumping ions to maintain the ionic gradients of the photoreceptors.[42] Because of the hyperpolarizing response of rods, exposure to bright light actually decreases ATP consumption by approximately 75%, despite the increased demand for ATP by the phototransduction components.[43] In the dark-adapted state, arrestin1 primarily concentrates in the inner segments where enolase1 is most abundant and would thus have an inhibitory effect on the glycolytic rate.[42,43] In response to light, most of the arrestin1 translocates to the outer segments, which would reduce the interaction with enolase1 in the inner segments and thus potentially increase the glycolytic rate when metabolic demand in terms of ATP is declining.

In light of this apparent contradiction, the interaction between arrestin and enolase1 may have more to do with the other arm of glycolysis—NADH production—than with supplying high energy ATP. NADH/NADPH is essential for the reduction of all-*trans* retinal produced by photoisomerization of 11-*cis* retinal in rhodopsin and subsequent suppression of quantum noise.[44] The upregulation of glycolysis by the translocation of arrestin1 away from enolase1 could provide additional NADH to facilitate this reduction of all-*trans* retinal. Another possibility for the interaction may be that arrestin1 serves as a scaffold in the dark-adapted state, building a complex of interactions that may relate to some as yet unidentified secondary function for enolase1 or other component of the complex. Arrestin's function as a scaffolding agent has been well recognized for the β-arrestins (arrestin2 and -3) (reviewed in Ref. 45) and more recently for arrestin1.[20]

The Role of Enolase1 in Arrestin Translocation

These studies have identified an interaction of arrestin1 with enolase1, a protein that is principally (>90%) localized to the inner segment region. Could enolase1 be the binding partner that attracts arrestin1 and -4 to the inner segments during dark adaptation? At this point, the evidence is not conclusive, identifying only a binding interaction between two proteins that are in the right location in dark-adapted photoreceptors. Perhaps importantly, the cytosolic distribution of enolase1 matches that of arrestin much better than that of microtubules. Only additional studies will reveal whether enolase1 or tubulin (or both) serves as the binding sink that maintains arrestin in the inner segments in dark-adapted photoreceptors.

In summary, our studies provide the first evidence for direct interaction between enolase1 and arrestin1 and -4. The colocalization of arrestin1 and enolase1 in the inner segments of dark-adapted rod photoreceptors, coupled with the demonstrated modulation of enolase1 enzymatic activity by arrestin1, suggests an important role for this interaction in the retina.

Acknowledgments

The authors thank Eric Roush (GE Healthcare) for assistance with developing the SPR assay.

References

1. Gurevich VV, Gurevich EV. The molecular acrobatics of arrestin activation. *Trends Pharmacol Sci.* 2004;25:105–111.
2. Peterson JJ, Tam BM, Moritz OL, et al. Arrestin migrates in photoreceptors in response to light: a study of arrestin localization using an arrestin-GFP fusion protein in transgenic frogs. *Exp Eye Res.* 2003;76:553–563.
3. Strissel KJ, Sokolov M, Trieu LH, Arshavsky VY. Arrestin translocation is induced at a critical threshold of visual signaling and is superstoichiometric to bleached rhodopsin. *J Neurosci.* 2006;26:1146–1153.
4. Whelan JP, McGinnis JF. Light-dependent subcellular movement of photoreceptor proteins. *J Neurosci Res.* 1988;20:263–270.
5. Zhang HB, Cuenca N, Ivanova T, et al. Identification and light-dependent translocation of a cone-specific antigen, cone arrestin, recognized by monoclonal antibody 7G6. *Invest Ophthalmol Vis Sci.* 2003;44:2858–2867.
6. Zhang HB, Huang W, Zhang HK, et al. Light-dependent redistribution of visual arrestins and transducin subunits in mice with defective phototransduction. *Mol Vis.* 2003;9:231–237.
7. Broekhuyse RM, Tolhuizen EFJ, Janssen APM, Winkens HJ. Light induced shift and binding of S-antigen in retinal rods. *Curr Eye Res.* 1985;4:613–618.
8. Philp NJ, Chang W, Long K. Light-stimulated protein movement in rod photoreceptor cells of the rat retina. *FEBS Lett.* 1987;225:127–132.
9. Zhu X, Li A, Brown B, Weiss ER, Osawa S, Craft CM. Mouse cone arrestin expression pattern: light induced translocation in cone photoreceptors. *Mol Vis.* 2002;8:462–471.
10. Elias R, Sezate S, Cao W, McGinnis J. Temporal kinetics of the light/dark translocation and compartmentation of arrestin and alpha-transducin in mouse photoreceptor cells. *Mol Vis.* 2004;10:672–681.
11. Nair KS, Hanson SM, Mendez A, et al. Light-dependent redistribution of arrestin in vertebrate rods is an energy-independent process governed by protein-protein interactions. *Neuron.* 2005;46:555–567.
12. Slepak VZ, Hurley JB. Mechanism of light-induced translocation of arrestin and transducin in photoreceptors: interaction-restricted diffusion. *IUBMB Life.* 2008;60:2–9.
13. Peet JA, Bragin A, Calvert PD, et al. Quantification of the cytoplasmic spaces of living cells with EGFP reveals arrestin-EGFP to be in

disequilibrium in dark adapted rod photoreceptors. *J Cell Sci.* 2004;117:3049–3059.

14. Calvert PD, Strissel KJ, Schiesser WE, Pugh JEN, Arshavsky VY. Light-driven translocation of signaling proteins in vertebrate photoreceptors. *Trends Cell Biol.* 2006;16:560–568.
15. Orisme W, Li J, Goldmann T, Bolch S, Wolfrum U, Smith WC. Light-dependent translocation of arrestin in rod photoreceptors is signaled through a phospholipase C cascade and requires ATP. *Cell Signal.* 2010;22:447–456.
16. Peterson JJ, Orisme W, Fellows J, et al. A role for cytoskeletal elements in the light-driven translocation of proteins in rod photoreceptors. *Invest Ophthalmol Vis Sci.* 2005;46:3988–3998.
17. Reidel B, Goldmann T, Giessl A, Wolfrum U. The translocation of signaling molecules in dark adapting mammalian rod photoreceptor cells is dependent on the cytoskeleton. *Cell Motil Cytoskel.* 2008;65:785–800.
18. Nair KS, Hanson SM, Kennedy MJ, Hurley JB, Gurevich VV, Slepak VZ. Direct binding of visual arrestin to microtubules determines the differential subcellular localization of its splice variants in rod photoreceptors. *J Biol Chem.* 2004;279:41240–41248.
19. Hanson SM, Francis DJ, Vishnivetskiy SA, Klug CS, Gurevich VV. Visual arrestin binding to microtubules involves a distinct conformational change. *J Biol Chem.* 2006;281:9765–9772.
20. Hanson SM, Cleghorn WM, Francis DJ, et al. Arrestin mobilizes signaling proteins to the cytoskeleton and redirects their activity. *J Mol Biol.* 2007;368:375–387.
21. McGinnis JF, Matsumoto B, Whelan JP, Cao W. Cytoskeleton participation in subcellular trafficking of signal transduction proteins in rod photoreceptor cells. *J Neurosci Res.* 2002;67:290–297.
22. Nir I, Ransom N. Ultrastructural analysis of arrestin distribution in mouse photoreceptors during dark/light cycle. *Exp Eye Res.* 1993; 57:307–318.
23. Smith WC. A splice variant of arrestin from human retina. *Exp Eye Res.* 1996;62:585–592.
24. Smith WC, Milam AH, Dugger DR, Arendt A, Hargrave PA, Palczewski K. A splice variant of arrestin: molecular cloning and localization in bovine retina. *J Biol Chem.* 1994;269:15407–15410.
25. Xiao K, McClatchy DB, Shukla AK, et al. Functional specialization of beta2-arrestin interactions revealed by proteomic analysis. *Proc Nat Acad Sci USA.* 2007;104:12011–12016.
26. Keller A, Nesvizhskii AI, Kolker E, Aebersold R. Empirical statistical model to estimate the accuracy of peptide identifications made by MS/MS and database search. *Anal Chem.* 2002;74:5383–5392.
27. Nesvizhskii AI, Keller A, Kolker E, Aebersold R. A statistical model for identifying proteins by tandem mass spectrometry. *Anal Chem.* 2003;75:4646–4658.
28. Buczylko J, Palczewski K. Purification of arrestin from bovine retinas. In: Hargrave PA, ed. *Photoreceptor Cells*. New York: Academic Press; 1993;15:226–236.
29. Puig J, Arendt A, Tomson FL, et al. Synthetic phosphopeptide from rhodopsin sequence induces retinal arrestin binding to photoactivated unphosphorylated rhodopsin. *FEBS Lett.* 1995;362:185–188.
30. McDowell JH, Smith WC, Miller RL, et al. Sulfhydryl reactivity demonstrates different conformational states for arrestin, arrestin activated by a synthetic phosphopeptide, and constitutively active arrestin. *Biochemistry.* 1999;38:6119–6125.
31. Smith WC, Dinculescu A, Peterson JJ, McDowell JH. The surface of visual arrestin that binds to rhodopsin. *Mol Vis.* 2004;10:392–398.
32. Bergmeyer HU. *Methods in Enzymatic Analysis*. 2nd ed. Vol. 2. 1974:449.
33. Palczewski K, Buczylko J, Ohguro H, et al. Characterization of a truncated form of arrestin isolated from bovine rod outer segments. *Prot Sci.* 1994;3:314–324.
34. Hamm HE, Bownds MD. Protein complement of rod outer segments of frog retina. *Biochemistry.* 1986;25:4512–4523.
35. Hanson SM, Gurevich EV, Vishnivetskiy SA, Ahmed MR, Song X, Gurevich VV. Each rhodopsin molecule binds its own arrestin. *Proc Nat Acad Sci USA.* 2007;104:3125–3128.
36. Hanson SM, Van Eps N, Francis DJ, et al. Structure and function of the visual arrestin oligomer. *EMBO J.* 2007;26:1726–1736.
37. Mirshahi MM, Camoin L, Nicolas C, Ghedira I, Cozette J, Faure JP. Copurification of selected glycolytic enzymes with retinal S-antigen (arrestin) by hydroxyapatite agarose chromatography of bovine retina. *Curr Eye Res.* 1999;18:327–334.
38. Hsu SC, Molday RS. Glycolytic enzymes and a GLUT-1 glucose transporter in the outer segments of rod and cone photoreceptor cells. *J Biolog Chem.* 1991;266:21745–21752.
39. Feo S, Arcuri D, Piddini E, Passantino R, Giallongo A. ENO1 gene product binds to the c-myc promoter and acts as a transcriptional repressor: relationship with Myc promoter-binding protein 1 (MBP-1). *FEBS Lett.* 2000;473:47–52.
40. Huang S-P, Brown BM, Craft CM. Visual arrestin 1 acts as a modulator for N-ethylmaleimide-sensitive factor in the photoreceptor synapse. *J Neurosci.* 2010;30:9381–9391.
41. Pancholi V. Multifunctional alpha-enolase: its role in diseases. *Cell Mol Life Sci.* 2001;58:902–920.
42. Okawa H, Sampath AP, Laughlin SB, Fain GL. ATP consumption by mammalian rod photoreceptors in darkness and in light. *Curr Biol.* 2008;18:1917–1921.
43. Winkler BS, Starnes CA, Twardy BS, Brault D, Taylor RC. Nuclear magnetic resonance and biochemical measurements of glucose utilization in the cone-dominant ground squirrel retina. *Invest Ophthalmol Vis Sci.* 2008;49:4613–4619.
44. Miyagishima KJ, Cornwall MC, Sampath AP. Metabolic constraints on the recovery of sensitivity after visual pigment bleaching in retinal rods. *J Gen Physiol.* 2009;134:165–175.
45. Kovacs JJ, Hara MR, Davenport CL, Kim J, Lefkowitz RJ. Arrestin development: emerging roles for β-arrestins in developmental signaling pathways. *Dev Cell.* 2009;17:443–458.